UC Berkeley
Research Reports

Title

Mixed Manual/Semi-Automated Traffic: A Macroscopic Analysis

Permalink

https://escholarship.org/uc/item/57x5x55b

Authors

Bose, Arnab

Ioannou, Petros

Publication Date

2001-04-01

Mixed Manual/Semi-Automated Traffic: A Macroscopic Analysis

Arnab Bose, Petros Ioannou
University of Southern California

CALIFORNIA PARTNERS FOR ADVANCED TRANSIT AND HIGHWAYS

Mixed Manual/Semi-Automated Traffic: A Macroscopic Analysis[*]

Arnab Bose and Petros Ioannou
Center for Advanced Transportation Technologies
Dept. of Electrical Engineering-Systems, EEB200B
University of Southern California
Los Angeles, CA 90089-2562, USA
abose@usc.edu, ioannou@almaak.usc.edu

Abstract

The use of advanced technologies and intelligence in vehicles and infrastructure could make the current highway transportation system much more efficient. Semi-automated vehicles with the capability of automatically following a vehicle in front as long as it is in the same lane and in the vicinity of the forward looking ranging sensor are expected to be deployed in the near future. Their penetration into the current manual traffic will give rise to mixed manual/semi-automated traffic. In this paper, we analyze the fundamental flow-density curve for mixed traffic using flow-density curves for 100% manual and 100% semi-automated traffic. Assuming that semi-automated vehicles use a time headway smaller than today's manual traffic average due to the use of sensors and actuators, we have shown using the flow-density diagram that the traffic flow rate will increase in mixed traffic. We have also shown that the flow-density curve for mixed traffic is restricted between the flow-density curves for 100% manual and 100% semi-automated traffic. We have presented in a graphical way that the presence of semi-automated vehicles in mixed traffic propagates a shock wave faster than in manual traffic. We have demonstrated that the presence of semi-automated vehicles does not change the total travel time of vehicles in mixed traffic. Though we observed that with 50% semi-automated vehicles a vehicle travels 10.6% more distance than a vehicle in manual traffic for the same time horizon and starting at approximately the same position, this increase is marginal and is within the modeling error. Lastly, we have shown that when shock waves on the highway produce stop-and-go traffic, the average delay experienced by vehicles at standstill is lower in mixed traffic than in manual traffic, while the average number of vehicles at standstill remains unchanged.

Executive Summary

In this paper, we present a macroscopic analysis of mixed manual/semi-automated traffic. We focus our analysis on two topics: the fundamental traffic flow-density diagram and traffic flow disturbances such as shock waves. We derive the fundamental traffic flow-density diagram for mixed manual/semi-automated traffic using the traffic flow-density diagrams for 100% manual and 100% semi-automated traffic. We show in a graphical way and demonstrate using simulations, the effect of semi-automated vehicles on mixed traffic flow during the presence of disturbances such as shock waves. Lastly, we show using queuing theory the effect of semi-automated vehicles on the average delay and number of vehicles in a queue on the highway during the presence of shock waves that produce stop-and-go traffic.

Contents

List of Figures

1 Introduction

During the past decade, researchers have focussed on improving traffic flow conditions with the help of automation. Several concepts that have been proposed include automation in the driver-vehicle system or the infrastructure or both. While fully automated vehicles on dedicated highways are seen as a far in the future objective, the use of partial or semi-automated vehicles on current highways with manually driven vehicles is deemed as a near-term goal.

Semi-automated vehicles are those that have the capability of automatically following a vehicle in front as long as it is in the same lane and within the range of the forward looking ranging sensor [6]. The vehicles use a longitudinal controller such as the Intelligent Cruise Control (ICC) system that comprises of throttle and brake subsystems [3]. The external input variables used by the ICC vehicle are the relative speed and the relative distance between itself and the leading vehicle (if any), in addition to its own speed obtained using different sensors [9]. It should be noted that ICC is also often referred to as Adaptive Cruise Control (ACC). Since the name, ACC could be confused with ordinary cruise control based on adaptive control also referred to as ACC we chose to use the name ICC in this report and past publications.

The use of sensors and actuators makes it possible for semi-automated vehicles to have a lower reaction time than manually driven vehicles. As a result, a semi-automated vehicle uses smaller time headway than current manual traffic average and reacts almost instantaneously to a speed differential in comparison to a manual vehicle. Time headway is the time taken to cover the distance between the rear of the front vehicle to the front of the following vehicle. Human factor considerations demand that the response of an ICC vehicle be smooth for passenger comfort. Hence, a semi-automated vehicle acts as a filter that smoothes out traffic flow disturbances [12]. The principle question is what will be the effect of the gradual penetration of semi-automated vehicles among manual ones on the mixed traffic flow, especially during the presence of disturbances.

In this paper, we focus our attention to the macroscopic analysis of mixed traffic flow. Two topics addressed are fundamental flow-density diagrams and shock waves. A fundamental flow-density diagram defines the steady-state relation between the traffic flow rate and the traffic density [1]. It is dependent on factors under which the traffic flow rate and the traffic density are observed like the length of time interval over which data is aggregated [11]. We outline flow-density diagrams for 100% manual and 100% semi-automated traffic. A linear follow-the-leader human driver model is used to model the dynamics of manually driven vehicles [2,7,11,16]. The model assumes that the human driver observes only the vehicle in front and sets its vehicle acceleration depending on the relative speed and the relative distance. A manual traffic flow-density curve is constructed using this human driver model. It has a stationary point that corresponds to maximum manual traffic flow rate. A flow-density curve for 100% semi-automated vehicles is constructed using the ICC design given in [3]. The highest point of the curve corresponds to maximum semi-automated traffic flow rate. We show using these flow-density curves that for any given traffic density, mixed traffic flow rate is greater than

1

manual traffic flow rate. We also show that the mixed traffic flow-density curve is restricted in the region encapsulated by these curves. As the percentage of semi-automated vehicles increases, this curve converges to the flow-density curve for 100% semi-automated traffic.

The effect of semi-automated vehicles among manual ones during the presence of traffic flow disturbances such as shock waves is shown using space-time diagrams and demonstrated using simulations. Shock waves are discontinuous waves that occur when traffic on a section of a road is denser in front and less dense behind. We present in a graphical way that the presence of semi-automated vehicles in mixed traffic propagates a shock wave faster than in manual traffic. We demonstrate that a vehicle in mixed traffic with 50% semi-automated vehicles travels 10.6% more distance than a vehicle in manual traffic for the same time horizon and starting at approximately the same position. A linear follow-the-leader human driver model, namely Pipes model [7,8] has been validated to closely model current manual driving [20]. Hence, it is used to model the dynamics of manual vehicles during the simulations. A three-dimensional representation of space-time diagrams is used to show that the traffic flow rate and the traffic density in mixed traffic are greater than that in manual traffic.

Lastly, we show that when shock waves produce stop-and-go traffic on the highway, the average delay experienced by vehicles is lower in mixed traffic than in manual traffic, while the average number of vehicles at standstill remains unchanged.

This paper is organized as follows: Section 2 introduces the traffic flow variables and analyzes mixed traffic flow using flow-density diagrams for 100% manual, 100% semi-automated and mixed traffic. Section 3 deals with shock waves and the effect of semi-automated vehicles on them. Section 4 compares the average delay experienced by vehicles during stop-and-go conditions on the highway in manual and mixed traffic. A summary of the main results is provided in the concluding Section 5.

2 Fundamental Flow-Density Diagram

Traffic flow rate q and traffic density k are average measures of traffic flow characteristics. The precise definition of q and k and the means of measuring them are explained in [1]. In this Section, we consider the flow-density diagrams for 100% manual traffic, 100% semi-automated traffic and analyze the flow-density curve for mixed manual/semi-automated traffic. A fundamental flow-density diagram defines the steady-state relation between the traffic flow rate and the traffic density [1]. It is dependent on factors under which the traffic flow rate and the traffic density are observed like the length of time interval over which data is aggregated [11].

2.1 Manual Traffic

A linear car-following model is used to model the motion of a manual vehicle. The car-following theory assumes that traffic stream is a superposition of vehicle pairs where

each vehicle follows the vehicle ahead according to some specific stimulus-response equation [2,7,16]. Using Fig. 1 we have the acceleration of the $(n+1)$-th vehicle given by [11]

$$\ddot{x}_{n+1}(t+\tau) = \lambda[\dot{x}_n(t) - \dot{x}_{n+1}(t)] \qquad (1)$$

where

τ : reaction time lag

λ : sensitivity factor and $\lambda = \lambda_0 \dfrac{\dot{x}^m_{n+1}(t+\tau)}{[x_n(t) - x_{n+1}(t)]^l}$

This is referred to as the (m, l) model. For $m=0$, $l=1.5$ we obtain

$$\ddot{x}_{n+1}(t+\tau) = \lambda_0 \frac{[\dot{x}_n(t) - \dot{x}_{n+1}(t)]}{[x_n(t) - x_{n+1}(t)]^{1.5}}$$

or,
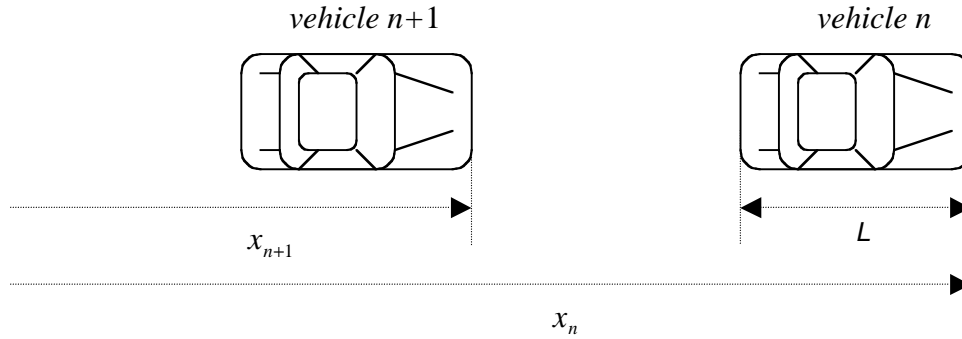
Figure 1: Vehicle following in a single lane.

$$\dot{v}_{n+1}(t+\tau) = \lambda_0 \frac{\dot{s}_{n+1}}{s_{n+1}^{1.5}}, \qquad (2)$$

where v_{n+1} : speed of $(n+1)$-th vehicle

$s_{n+1} = x_n(t) - x_{n+1}(t)$: intervehicle spacing of the $(n+1)$-th vehicle

The intervehicle spacing is defined as the distance between same points in successive vehicles.

To analyze the macroscopic effect we neglect the reaction time lag τ. In [11] it is shown that the time lag does not affect the equation that describes the macroscopic traffic flow behavior. Dropping the subscripts in (2) we get

3

$$\dot{v} = \lambda_0 \frac{\dot{s}}{s^{1.5}} \tag{3}$$

It can be shown that the reciprocal of the average intervehicle spacing is the traffic density [4]. Therefore, using $k = \dfrac{1}{s}$ where k represents the traffic density, we can express (3) as

$$\dot{v} = -\lambda_0 k^{1.5} \frac{\dot{k}}{k^2} \tag{4}$$

Integrating (4) we have

$$\int_{v}^{0} \dot{v} = -\lambda_0 \int_{k}^{k_j} \frac{\dot{k}}{k^{0.5}} \tag{5}$$

where the limits are from the present point (v,k) to the jam condition where all vehicles are at standstill, i.e. $v = 0$ and $k = k_j$, where k_j is the traffic density at jam condition. Evaluating (5) we get

$$v = 2\lambda_0 \left(\sqrt{k_j} - \sqrt{k} \right) \tag{6}$$

The proportionality constant λ_0 in (6) can be expressed in terms of speed and traffic density using $v = v_f$ when $k = 0$, i.e. when the density is negligible, there is no vehicle-to-vehicle interaction and vehicles travel at mean free speed v_f. The mean free speed is the vehicle speed that is not affected by other vehicles and only subjected to constraints associated with the vehicle and road characteristics. That gives us

$$\lambda_0 = \frac{v_f}{2\sqrt{k_j}}$$

Substituting for λ_0 in (6) we obtain the average speed of vehicles on a section of the road

$$v = v_f \left(1 - \sqrt{\frac{k}{k_j}} \right) \tag{7}$$

where

v_f : mean free speed that corresponds to negligible traffic density when there is no interaction among vehicles.

k : traffic density on the section of the road.

4

k_j : jam density equal to $1/L$ where L is the average length of vehicles, i.e. the traffic density corresponding to jam conditions when the vehicles are stacked bumper-to-bumper and the speed is zero.

The traffic flow rate q at steady state measures the number of vehicles moving in a specified direction on the road per unit time and is given by

$$q = kv \tag{8}$$

Substituting v from (7) we get an equation of the manual traffic flow-density relationship at steady state given by

$$q = kv = kv_f\left(1 - \sqrt{\frac{k}{k_j}}\right) \equiv Q(k) \tag{9}$$

which is also used to obtain the fundamental $q - k$ diagram shown in Fig. 2.

The speed of waves carrying continuous changes of flow along the vehicle stream is the slope of the tangent to the $q - k$ curve at a point and is given by

$$c = \frac{dq}{dk} = \frac{d(kv)}{dk} = v + k\frac{dv}{dk} \tag{10}$$

The wave speed is smaller than the average speed of the vehicles when the latter decreases with increase in traffic density, i.e. $\frac{dv}{dk} \leq 0$. The equality holds when the density is very low and any increase does not affect the average speed of the vehicles. Such conditions exist near the origin of the $q - k$ diagram where the density is negligible and there is no vehicle-to-vehicle interaction.

The $q - k$ curve has a stationary point that corresponds to a critical density k_{cm} that gives the maximum traffic flow rate q_{mm} or the capacity on the section of the road. The slope of the line joining a point on the $q - k$ curve to the origin gives the average speed of vehicles at that point. The equation (9) is an example of a flow-density model derived from the (m,l) model and is used to qualitatively describe manual traffic flow characteristics. Different values of m and l are used to obtain a good fit to actual traffic flow data. For example, in [1] it is mentioned that the flow-density model derived with m=0.8 and l=2.8 gives a good fit to data observed on an expressway in Chicago. The flow-density model derived using m=1 and l=3 is shown to be qualitatively valid for traffic flow characteristics observed in 3-lane Boulevard Pϑriphϑrique de Paris [16]. Likewise, m=0 and l=1 is used to derive a flow-density model that gives a good fit to actual traffic flow data taken in the Lincoln Tunnel in New York [17].

5

The point (q_{mm}, k_{cm}) has been empirically observed to be unstable, i.e. it leads to a breakdown in traffic flow. When traffic flow conditions exist at or near this point, the traffic flow and the average speed decreases as traffic density increases, and the operating point moves towards the jam density k_j on the $q - k$ curve. This observation is explained in [15]. As capacity is approached, flow tends to become unstable as the number of available gaps reduces. Traffic flow at capacity means that there are no usable gaps left. A disturbance in such a condition due to lane changing or vehicle merging is not 'effectively damped' or 'dissipated'. This leads to a breakdown in traffic flow and 'formation of upstream queues'. As pointed in [15], this is the reason why all facilities are designed to operate at lower than maximum traffic flow conditions.

2.2 Semi-Automated Traffic

While the behavior of human drivers is random and at best we can develop a manual traffic flow-density model that is qualitatively valid, the responses of semi-automated vehicles are deterministic due to the use of computerized longitudinal controllers. In this Section, we utilize this advantage along with certain assumptions to develop a deterministic semi-automated traffic flow-density model that is used to obtain the fundamental $q - k$ diagram. A semi-automated vehicle uses a longitudinal controller to automatically follow a vehicle in the same lane and within the range of its forward-looking ranging sensor. Many such controller designs exist in literature that use constant time headway [3,14] and constant spacing [13] policies. In this paper we consider the ICC design given in [3] which uses a constant time headway policy. The time headway is defined as the time taken to travel the distance between the rear end of the lead vehicle and the front end of the following vehicle.
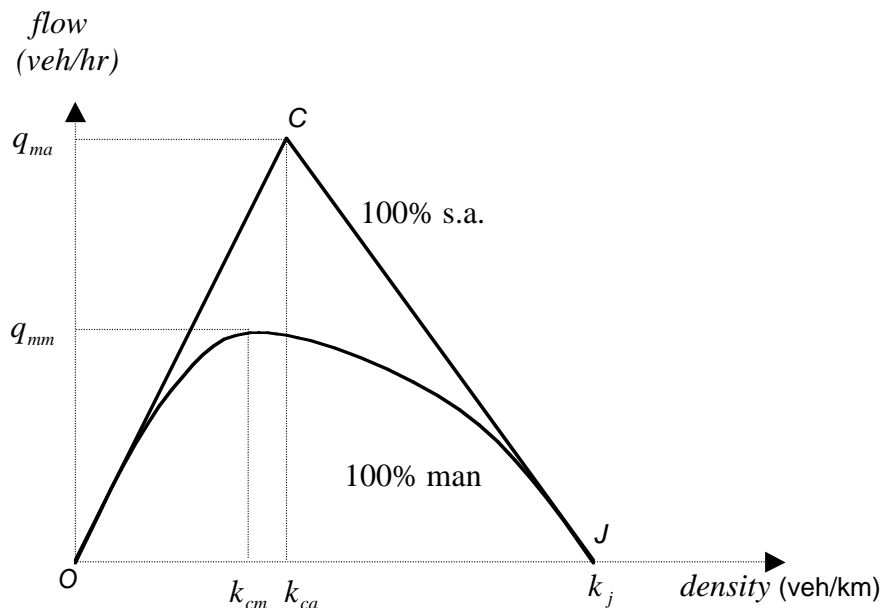

Figure 2: Fundamental flow-density curves for 100% manual traffic and 100% semi-automated traffic.

6

The intervehicle spacing s at a speed v followed by a semi-automated vehicle using constant time headway h_a is given by

$$s = h_a v + L \tag{11}$$

where L is the length of the vehicle. For simplicity, we assume that all semi-automated vehicles have the same length L and use the same time headway h_a.

The average intervehicle spacing is the reciprocal of traffic density. When traffic density is such that the intervehicle spacing is greater than or equal to that given by (11), then during this period at steady state the traffic flow rate given by (8) increases linearly with the density of semi-automated vehicles according to

$$q = kv_f$$

where v_f is the mean free speed. This situation is indicated by the line OC in Fig. 2.

As the traffic density increases and reaches the value

$$k = k_{ca} = \frac{1}{h_a v_f + L}$$

the maximum semi-automated traffic flow rate q_{ma} or capacity is reached. Thereafter, the relation between q and k can no longer change unless the speed v_f or the time headway h_a changes. We assume that the time headway h_a is fixed at all speeds[1] and further increase in k occurs due to changes in speed. In such a case we have

$$s = h_a v + L < h_a v_f + L \tag{12}$$

and

$$k = \frac{1}{h_a v + L} > k_{ca} = \frac{1}{h_a v_f + L} \tag{13}$$

Thus, the speed of the semi-automated vehicles decreases with increasing k according to

$$v = \frac{1}{h_a}\left(\frac{1}{k} - L\right) \tag{14}$$

The traffic flow rate is given by

---

[1] This is reasonable as the purpose of ICC is to maintain a fixed time headway at all speeds. It is possible, however, that the driver may manually change the time headway, as some ICC systems already deployed have this option. In our analysis, we did not model such driver responses.

$$q = kv = \frac{1}{h_a}(1 - kL)$$

Graphically, the slope of the line joining the origin to a point on the $q - k$ curve gives the speed of the semi-automated vehicles at that point. It can be seen that before the critical density the speed remains constant at v_f. After reaching the critical density k_{ca}, the speed falls as the traffic density increases (Fig. 2).

Therefore, the steady state fundamental flow-density diagram for 100% semi-automated traffic is given by

$$q = \begin{cases} kv_f & k \le k_{ca} \\ \dfrac{1}{h_a}(1 - kL) & k > k_{ca} \end{cases} \tag{15}$$

Equation (15) describes the average steady state traffic flow characteristics. They do not capture any effects due to individual vehicle responses.

In region OC of the $q - k$ curve, the critical density is not yet reached. The average speed of the semi-automated vehicles is equal to the mean free speed v_f. This region corresponds to "loose" vehicle following where some semi-automated vehicles travel without following any vehicle and use an intervehicle spacing greater than that given by (11). The rest follow a lead vehicle and use an intervehicle spacing given by (11). After C the average speed of the semi-automated vehicles along with the traffic flow rate begin to decrease with increase in density. This region indicated by the line CJ corresponds to "tight" vehicle following where all semi-automated vehicles follow a lead vehicle and use an intervehicle spacing given by (12). Finally, at maximum density k_j all semi-automated vehicles are at dead stop and stacked bumper-to-bumper.

Let us now consider the stability of the point (q_{ma}, k_{ca}). We mentioned in the previous subsection that the corresponding point (q_{mm}, k_{cm}) in manual traffic has been empirically observed to be unstable. Obviously, it is not possible to empirically determine the stability of (q_{ma}, k_{ca}). However, it is expected that the point (q_{ma}, k_{ca}) will also be unstable, i.e. at this operating point, there will be a breakdown in traffic flow. As in manual traffic, flow will tend to become unstable as capacity is approached and the number of available gaps reduces. At critical density there will be no usable gaps left. Any disturbance generated at this condition is expected to lead to the formation of upstream queues and a breakdown in traffic flow, as observed in manual traffic. Furthermore, it has been shown that traffic flow in the region CJ where the intervehicle spacing is given by (13) is unstable in the sense that disturbances propagate upstream unattenuated [21].

2.3 Mixed Manual/Semi-Automated Traffic

In the previous subsections, at one end we developed a flow-density model that qualitatively describes manual traffic flow characteristics. At the other end, we developed a deterministic flow-density model for semi-automated traffic. A combination of these two models is expected to characterize mixed manual/semi-automated traffic flow, which we analyze in this Section.

We assume that at steady state conditions vehicles of the same class use identical time headways. For semi-automated vehicles, this is equal to the designed value of the ICC controller. For manual vehicles, we take it to be equal to the average value observed in current manual traffic. This is done for simplicity of analysis and it does not affect the qualitative nature of the results.
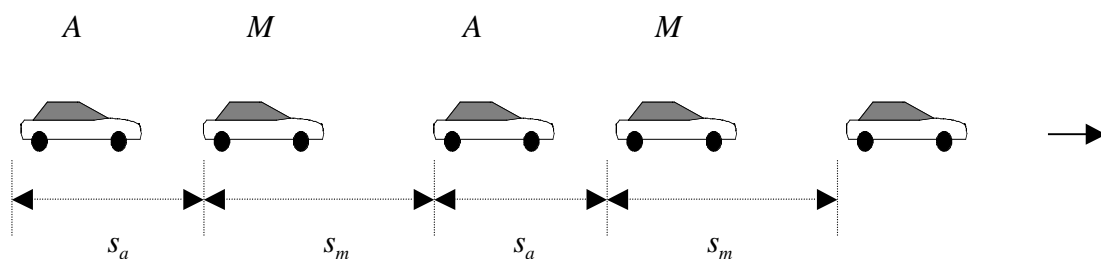

Figure 3: Mixed manual/semi-automated traffic.

Consider the mixed traffic flow shown in Fig. 3. Manual vehicles are marked '*M*' and semi-automated vehicles are marked '*A*'. Assuming moderately dense traffic conditions, the average vehicle spacing defined as the distance between the two rear ends of two consecutive vehicles at steady state conditions is given by

$$\bar{s} = ps_a + (1-p)s_m \qquad (16)$$

where

p: market penetration of semi-automated vehicles in mixed traffic.

$s_a = h_a v + L$: vehicle spacing used by semi-automated vehicles at speed v with time headway h_a; L is the average length of the vehicle.

$s_m = h_m v + L$: average vehicle spacing used by manual vehicles at speed v for a time headway h_m which is the average of current manual traffic time headway distribution.

Remark 1: Throughout this paper, we assume that due to the use of sensors and actuators in semi-automated vehicles, $h_a < h_m$, i.e. $s_a < s_m$ at a given speed and for the same average length of manual and semi-automated vehicles [6].

The total mixed traffic density is given by

9

$$k_{mix} = \frac{1}{\bar{s}} \equiv f(p, s_a, s_m) \tag{17}$$

We assume that the driver of a manual vehicle behaves the same way whether following a semi-automated vehicle or a manual vehicle. Under this assumption, we can use the fundamental flow-density curve for 100% manual traffic to determine the characteristics of manual vehicles in mixed traffic. Likewise, the flow-density curve for 100% semi-automated traffic can be used for semi-automated vehicles in mixed traffic, as their vehicle dynamics remain unchanged when following a manually driven vehicle.

The steady state speed of mixed traffic is determined by the speed of the slowest moving vehicle class (manual or semi-automated). Using the above assumption, we take the inverse of the average intervehicle spacing for each vehicle class as their density, i.e. $k_m = \frac{1}{s_m}$ and $k_a = \frac{1}{s_a}$. Then use (7) and (14) to determine the average speeds at which the manual and the semi-automated vehicles can travel. The lower of the two determines the speed at which all vehicles travel in mixed traffic. Note that from (17) the density of each class is dependent on the other.

Lemma 1: The $q - k$ curve for mixed manual/semi-automated traffic remains in the region between the $q - k$ curves for 100% manual and 100% semi-automated traffic. Furthermore, the mixed traffic flow rate is greater than the manual traffic flow rate for the same traffic density.

Proof:

Case 1: $v_a > v_m$

This means that the average steady state mixed traffic speed is $v_{mix} = v_m$. Now the intervehicle spacing followed by the semi-automated vehicles is given by

$$s_a = h_a v_a + L \tag{18}$$

and the corresponding density is $k_a = \frac{1}{s_a}$, which is the point o_1 in the fundamental diagram in Fig. 4. Likewise, the intervehicle spacing for the manual vehicles is given by

$$s_m = h_m v_m + L \tag{19}$$

and the density is $k_m = \frac{1}{s_m}$, the point o_2 in the fundamental diagram. Now as the total traffic travels at average speed v_m, then (18) changes to
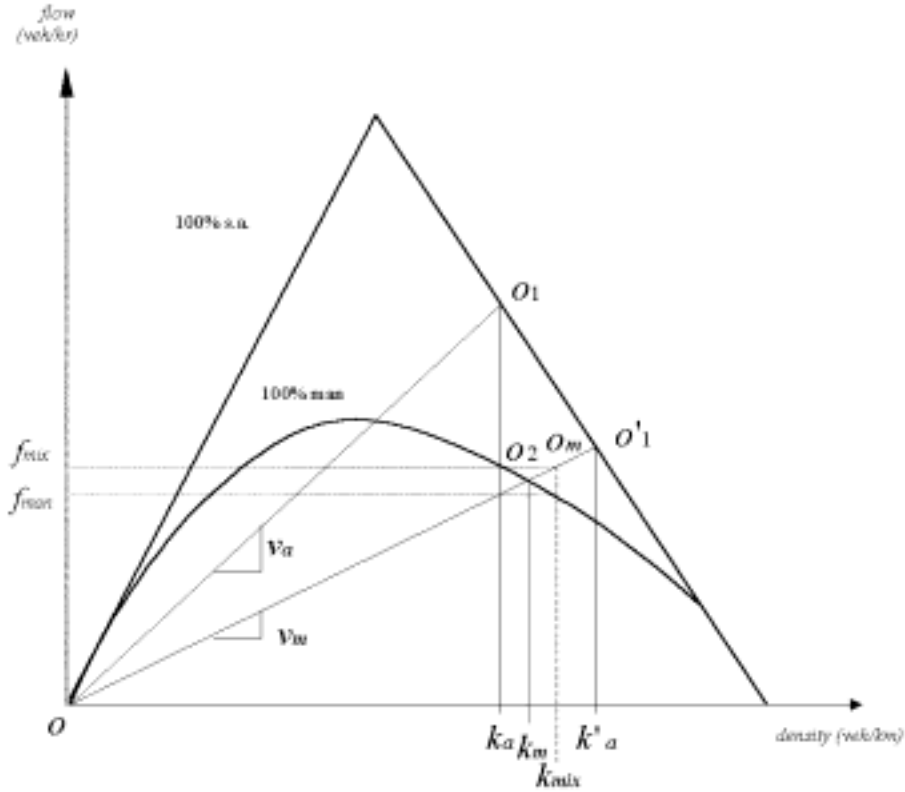
$$s_a' = h_a v_m + L \tag{20}$$

10

Figure 4: Derivation of a mixed traffic $q - k$ operating point when the manual vehicles set the average steady state speed.

and the new density is given by $k'_a = \dfrac{1}{s'_a}$, which corresponds to the point o'_1 in the fundamental diagram. The density of the mixed traffic by Remark 1 always satisfies

$$k_m < k_{mix} < k_a \tag{21}$$

Thus, the new point in the fundamental diagram of mixed traffic is given by o_m corresponding to mixed traffic flow rate f_{mix}.

Consider now 100% manual traffic at density k_{mix}. The manual traffic flow rate corresponding to that density is given by $f_{man} < f_{mix}$. Thus, we show that the mixed traffic flow rate is greater than the manual traffic flow rate for the same traffic density when the manual vehicles set the average mixed traffic speed at steady state.

Case 2: $v_a < v_m$

This means that the average steady state mixed traffic speed is $v_{mix} = v_a$. Now the intervehicle spacing followed by the semi-automated vehicles is given by

11

$$s_a = h_a v_a + L \tag{22}$$

and the corresponding density is $k_a = \dfrac{1}{s_a}$, which is the point o_2 in the fundamental diagram in Fig. 5. Likewise, the intervehicle spacing for the manual vehicles is given by

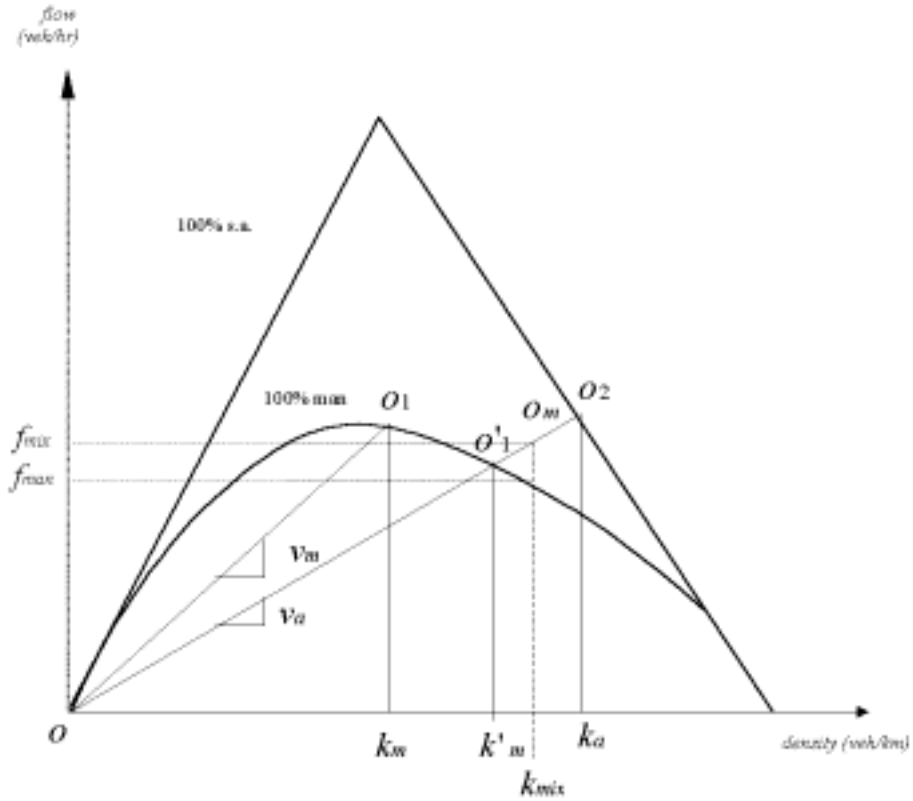$$s_m = h_m v_m + L \tag{23}$$

Figure 5: Derivation of a mixed traffic $q - k$ operating point when the semi-automated vehicles set the steady state average speed.

and the density is $k_m = \dfrac{1}{s_m}$, the point o_1 in the fundamental diagram. Now as the total traffic travels at average speed v_a, then (23) changes to

$$s'_m = h_m v_a + L \tag{24}$$

12

and the new density is given by $k'_m = \dfrac{1}{s'_m}$, which corresponds to the point o'_1 in the fundamental diagram. Using Remark 1 and (21) we show that mixed traffic point is given by o_m corresponding to mixed traffic flow rate f_{mix}.

Consider now 100% manual traffic at density k_{mix}. The manual traffic flow rate corresponding to that density is given by $f_{man} < f_{mix}$. Thus, we show that the mixed traffic flow rate is greater than the manual traffic flow rate for the same traffic density when the semi-automated vehicles set the average mixed traffic speed at steady state.
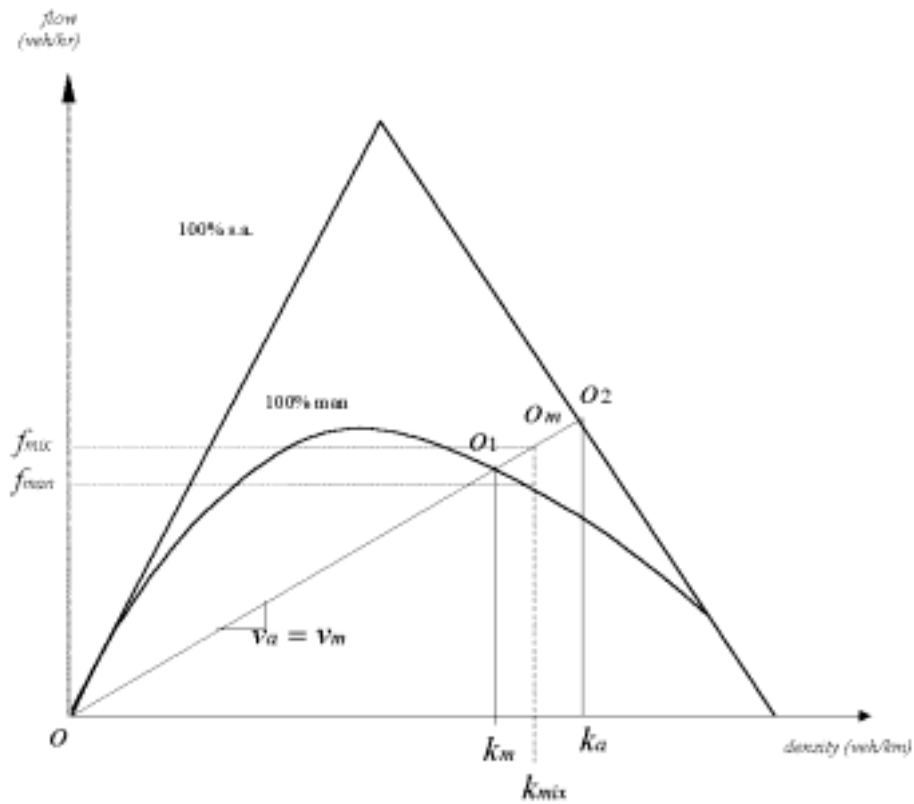
Case 3: $v_a = v_m$

Figure 6: Derivation of a mixed traffic $q - k$ operating point when the average speed of the semi-automated and the manual vehicles are the same at steady state.

This means that the average steady state mixed traffic speed is $v_{mix} = v_a = v_m$. Now the intervehicle spacing followed by the semi-automated vehicles is given by

$$s_a = h_a v_a + L \qquad (25)$$

and the corresponding density is $k_a = \dfrac{1}{s_a}$, which is the point o_2 in the fundamental diagram in Fig. 6. Likewise, the intervehicle spacing for the manual vehicles is given by

$$s_m = h_m v_m + L \tag{26}$$

and the density is $k_m = \dfrac{1}{s_m}$, the point o_1 in the fundamental diagram. Now as the total traffic travels at speed $v_a = v_m$, the operating point of the mixed traffic flow is given by o_m corresponding to mixed traffic density $k'_m = \dfrac{1}{s'_m}$ and mixed traffic flow rate f_{mix}.

Consider now 100% manual traffic at density k_{mix}. The manual traffic flow rate corresponding to that density is given by $f_{man} < f_{mix}$. Thus, we show that the mixed traffic flow rate is greater than the manual traffic flow rate for the same traffic density when the average speed of the semi-automated vehicles and the manual vehicles are the same at steady state.

◇

Lemma 1 and its proof give an insight into the evolution of mixed traffic. To observe the behavior of the mixed traffic $q - k$ curve operating point as the percentage p of semi-automated vehicles increases, we consider two separate cases:

Case 1 Assume that as p increases, the average speed is equal to the speed of the manual vehicles and $k_a \leq k_{ca}$. Then from (7) as the percentage of semi-automated vehicles increases, i.e. $p \to 1$, $k_m = k \to 0$ and $v \to v_f$. From (17) $k_{mix} \to k_a$ to give us

$$q = \lim_{p \to 1} k_{mix} v = k_a v_f \tag{27}$$

This is the same as (15) for $k_a \leq k_{ca}$.

Case 2 Assume that as p increases, the average speed is equal to the speed of the semi-automated vehicles. This means that $k_a > k_{ca}$. Otherwise the average speed of semi-automated vehicles will be v_f, the maximum for manual vehicles, which is not possible. Then from (14) as $p \to 1$, $v \to \dfrac{1}{h_a}\left(\dfrac{1}{k_a} - L\right)$ and from (17) $k_{mix} \to k_a$ to give us

$$q = \lim_{p \to 1} k_{mix} v = \frac{1}{h_a}(1 - k_a L) \tag{28}$$

This is the same as (15) for $k_a > k_{ca}$.

Thus, we observe how the $q - k$ curve for mixed traffic converges to the $q - k$ curve for 100% semi-automated traffic as the percentage of semi-automated vehicles increases.

Now we draw a $q - k$ curve for a given market penetration of semi-automated vehicles with the help of the analyses presented above. The initial points of the curve merge with the $q - k$ curves for 100% semi-automated and 100% manual traffic as seen in Fig. 7, denoting the region where all vehicles travel at mean free speed and there is no vehicle-to-vehicle interaction. Thereafter we trace the bivariate relationship for mixed traffic using the average intervehicle spacings used by the manual and the semi-automated vehicles as outlined previously. Each unique p corresponds to a unique mixed traffic $q - k$ curve.

Figure 7: Fundamental $q - k$ diagrams for 100% semi-automated, 100% manual and p mixed traffic at steady state conditions.

Lastly, we investigate the mixed traffic critical density. Each curve has a maximum traffic flow point that corresponds to the critical density. Therefore, the mixed traffic critical density depends on the combination of the intervehicle spacings s_a and s_m used

by the semi-automated and the manual vehicles, respectively. Furthermore, the operating point on the $q - k$ curve at critical density corresponding to maximum mixed traffic flow is expected to be unstable and lead to a breakdown in mixed traffic flow. Since at critical density there are no available gaps left, a phenomenon similar to that observed in manual traffic is expected to occur in the event of a traffic disturbance.

3 Shock Waves in Mixed Traffic

Shock waves are discontinuous waves that occur when traffic on a section of a road is denser in front and less dense behind. The waves on the less dense section travel faster than those in the dense section ahead and catch up with them. Then the continuous waves coalesce into a discontinuous wave or a 'shock wave' [1]. It can be shown that shock waves travel at a speed given by

$$u = \frac{\Delta q}{\Delta k} \tag{29}$$

where Δq and Δk are the traffic flow rate and traffic density differences, respectively, between the two sections. In the fundamental diagram for manual traffic, this is given by the slope of the chord joining the two points that represent conditions ahead and behind the shock wave at *a* and *b*, respectively (Fig. 8).
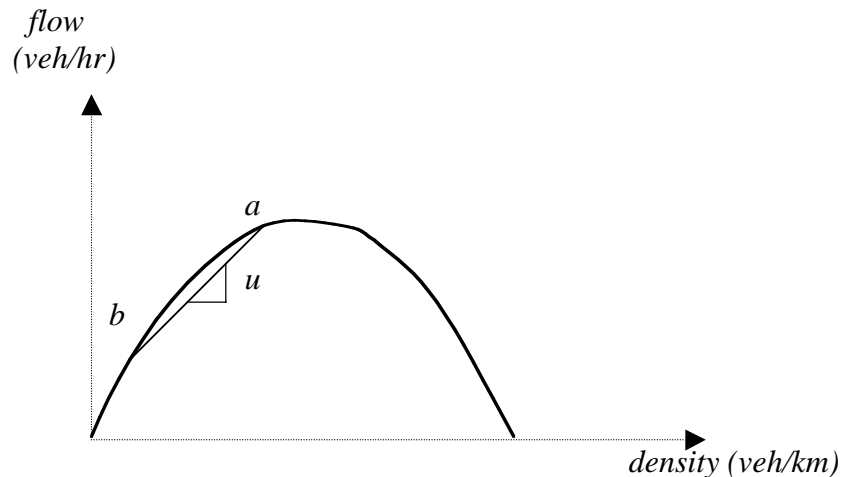

Figure 8: Shock wave in manual traffic.

The question that we pose is: how does the mixing of semi-automated and manual vehicles affect the shock waves? We answer the question using space-time diagrams that represent vehicle trajectories. This simple theory of traffic evolution will provide an insight into the effect of semi-automated vehicles among manually driven ones on the propagation of shock waves. The theory is also used in [4] and is a version of one originally developed in [1]. It is presented in a graphical way and assumes the following:

16

no overtaking and vehicles of the same class (i.e. manual and semi-automated) exhibit identical headways, spacings and velocities within a given state.

Figure 9(a) shows the space-time graph for 5 vehicles in manual traffic. At time instant, t_d a disturbance causes the lead vehicle to slow down, denoted by a change in slope in the diagram. We assume that the vehicle decelerations occur instantaneously. After a time lag τ, the following vehicle reacts and decelerates to maintain the intervehicle spacing depending on a constant time headway policy. Likewise, the rest of
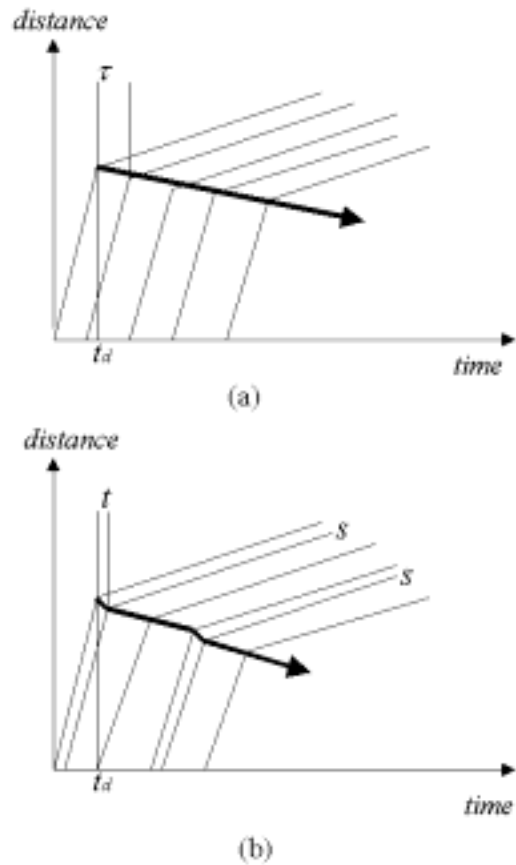

Figure 9: Space-time graph showing traffic evolution and the propagation of shock waves in (a) manual traffic and (b) mixed traffic.

the manual vehicles respond as shown. The shock wave that exists at the boundary of the two regions moves back at a speed given by the slope of the arrow in Fig. 9(a).

For mixed traffic shown in Fig. 9(b), the lines marked 's' denote semi-automated vehicles while the rest are manually driven ones. As before, the disturbance at t_d causes the first vehicle to slow down. The following semi-automated vehicle reacts after a time t, where t depends on the sensors and the actuators of the semi-automated vehicle and $t \ll \tau$, i.e. much smaller than the time lag for human drivers in manual vehicles. This

17

effect continues upstream with the semi-automated vehicles reacting almost instantaneously to speed changes while the manual vehicles have a time lag τ. As shown in Fig. 9(b), the resultant effect is that the average slope of the shock wave increases and as a result, it travels upstream at a higher speed than in Fig. 9(a).

This phenomenon is illustrated in a three-dimensional representation of the space-time diagram. We construct an axis of cumulative number of vehicles at three different distance points and at three different time instances. The surface of the cumulative vehicle count $N(x,t)$ is staircase-shaped, with each step representing a vehicle trajectory. It follows that if the surfaces are taken to be continuous, then the traffic flow rate at a given point can be obtained from the $N(x,t)-t$ diagrams directly by using

$$q_x(t) = \frac{\partial\ N(x,t)}{\partial\ t} \tag{30}$$

and the traffic density at a given time can be obtained from the $N(x,t)-x$ diagrams using

$$k_t(x) = -\frac{\partial\ N(x,t)}{\partial\ x} \tag{31}$$

We use a negative sign in (31) because the cumulative vehicle count is considered by counting the number of vehicles that have not yet crossed the line at a time instance t in the space-time diagrams. This is the number of vehicles to the left of t, which is opposite to the motion of the vehicles and hence the negative derivative.

It is important to note that the continuum approximation to a discrete flow is valid only in the regime of dense traffic. Writing (30) and (31) together, we obtain the continuity equation

$$\frac{\partial\ q}{\partial\ x} + \frac{\partial\ k}{\partial\ t} = 0 \tag{32}$$

The cumulative vehicle count curve $N(x_2,t)$ for the point x_2 in the $N(x,t)-t$ diagrams in Fig. 10 is obtained by shifting the curve $N(x_1,t)$ horizontally to the right by the time it takes a vehicle to travel from x_1 to x_2. However, this is not the proper representation of the cumulative curve at x_2 due to the presence of the shock wave. Thus, we perform the following transformations. We shift the cumulative curve $N(x_3,t)$ for x_3 (a point after the shock wave) horizontally to the right by the time it takes the shock wave to travel from x_3 to x_2, and vertically upwards by the number of vehicles that cross the shock wave interface. The number of vehicles that cross the shock wave interface is given by the product of traffic density in the region after the shock wave and the distance from x_2 to x_3. This curve is then combined with $N(x_2,t)$ to obtain the correct cumulative curve $N'(x_2,t)$ at x_2. We use a similar procedure to construct the cumulative
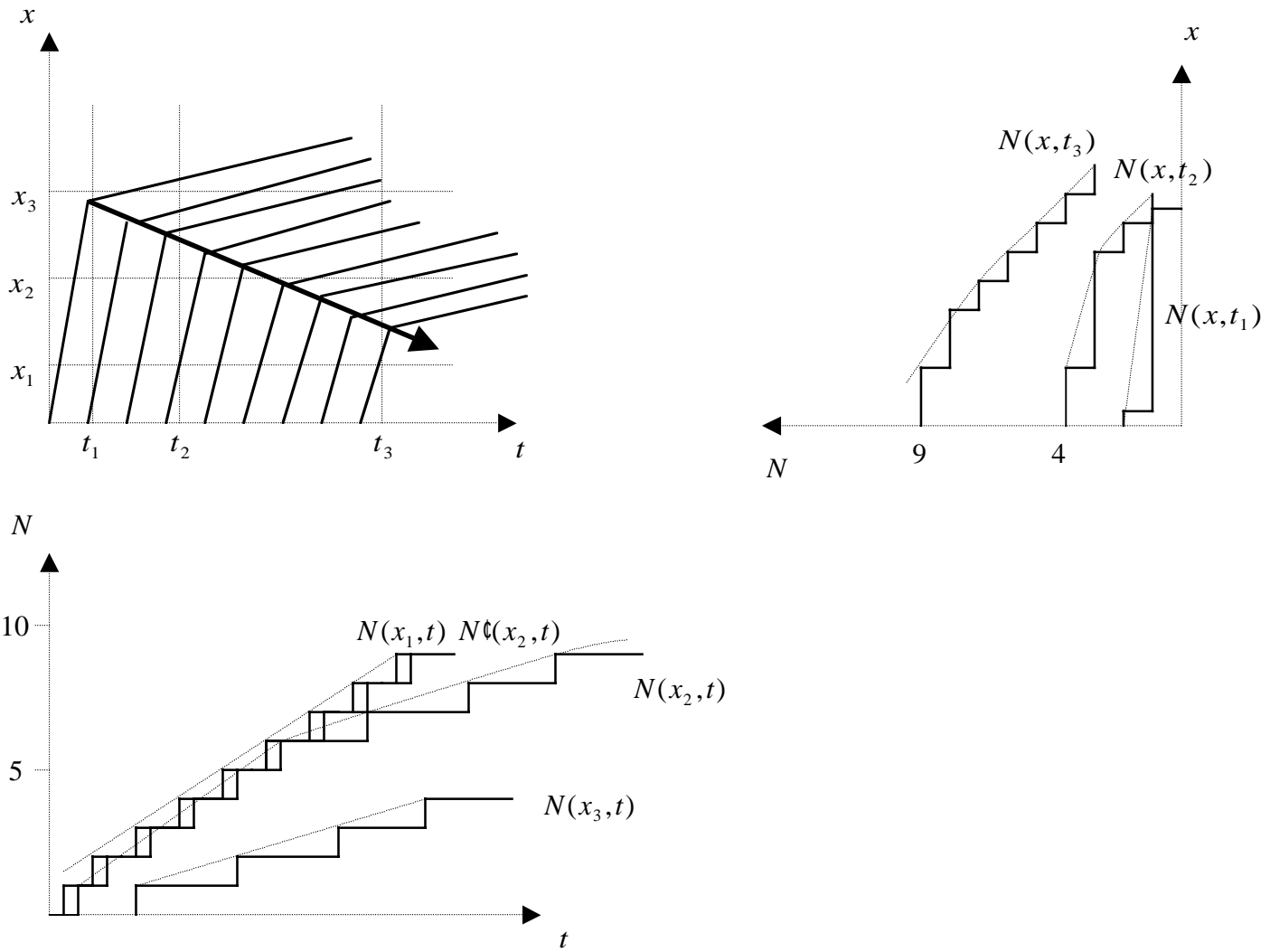
19

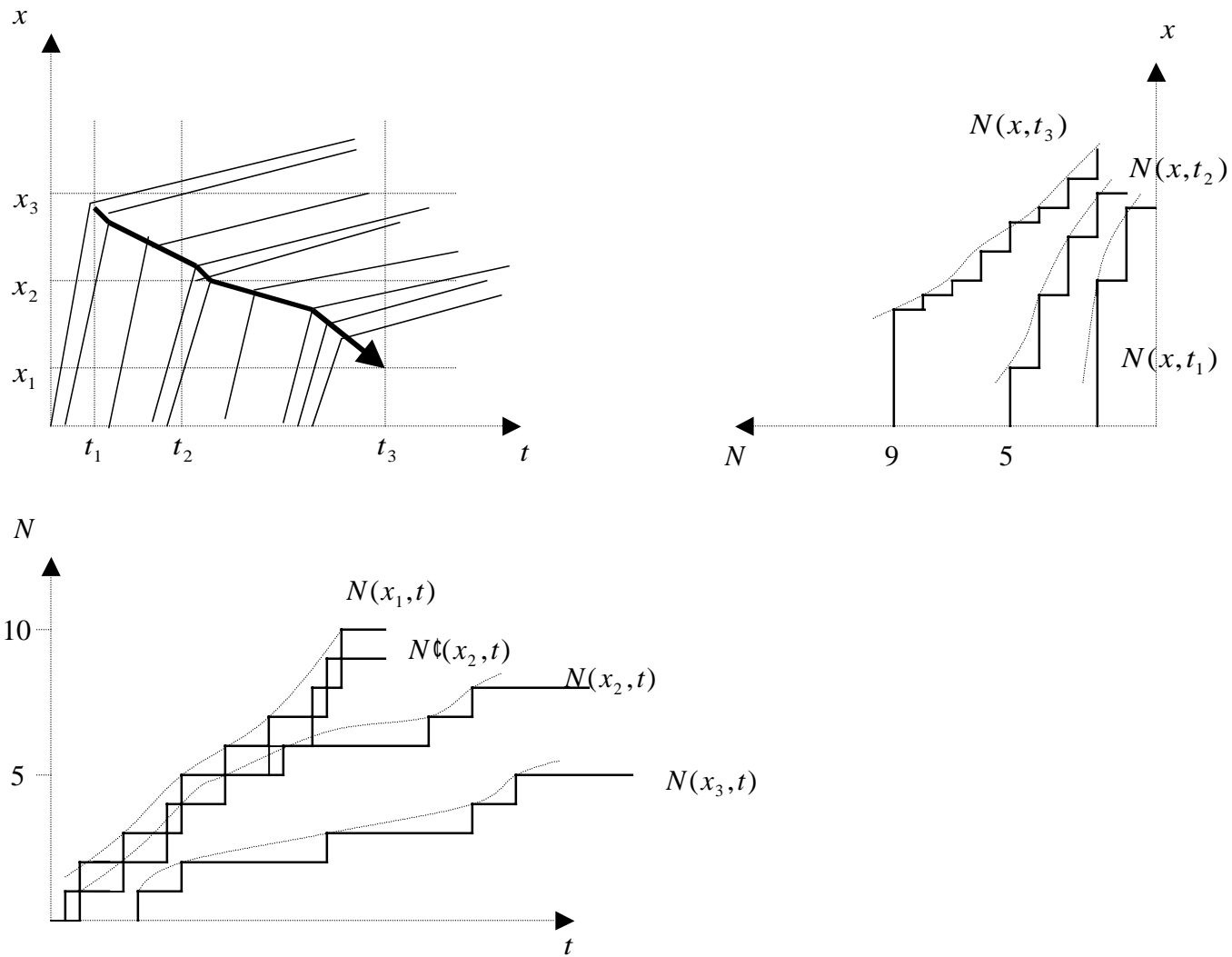Figure 10(a): Three-dimensional representation of manual traffic.

Figure 10(b): Three-dimensional representation of mixed traffic.

vehicle count curve $N(x,t_2)$ at time instant t_2 in $N(x,t)-x$ diagrams in Fig. 10. The cumulative N-curves are the ones that will be observed if vehicles counts are taken using measurement devices at positions x_1, x_2 and x_3 at time instances t_1, t_2 and t_3.

We observe from the cumulative curves in Fig. 10 that the traffic flow rate and the traffic density are greater in mixed traffic than in manual traffic. Furthermore, we observe from the $N(x,t)-t$ diagrams that the traffic flow rate at a given point decreases more rapidly in mixed traffic than in manual traffic. Likewise, from the $N(x,t)-x$ diagrams, we can conclude that the rate of increase in traffic density is higher in mixed traffic than in manual traffic. These are consequences of the shock wave travelling faster in mixed traffic than in manual traffic.

To demonstrate this we perform the following simulations for manual and mixed traffic. Consider a stretch of road of length 2.5 km subdivided into 5 sections of 500m each. A constant traffic flow rate is assumed along the road. The manual vehicle dynamics are modeled using the Pipes linear car-following model from [7,8] and the semi-automated vehicle dynamics are modeled using the ICC design presented in [3]. The Pipes linear car following and the ICC models have been validated using actual vehicle following experiments in [3,20]. All vehicles follow a constant time headway policy. The time headways for the manual vehicles are generated according to a lognormal distribution given in [5] while for semi-automated vehicles they are considered to be 1s. It is important to note that the time headway defined in [5] is the time taken to cover the distance that includes the vehicle length. The maximum value for the manual vehicle time headway is taken as 4s. This is done to make the study applicable to current manual traffic where seldom a vehicle in moderately dense traffic conditions uses a time headway greater than 4s. Fig. 11(a) shows the time headway of vehicles in 100% manual traffic on the road. Initially all vehicles are travelling at 15m/s. We introduce a disturbance in the 3rd section that lasts for 10s and results in all vehicles in that section to slow down to 5m/s. The average speed and traffic density of each section of the road for 50s are shown in Fig. 11(b) and 11(c), respectively. We observe a shock wave developing in section 3 that causes a pile-up of vehicles.

Next, we assume 50% semi-automated vehicles in mixed traffic that are placed randomly among manually driven vehicles on the road. The time headways for the vehicles are shown in Fig. 12(a). A similar disturbance is introduced that results in all vehicles in section 3 to slow down to 5m/s. We observe in Fig. 12(b) and 12(c) that the shock wave in section 3 moves back at a speed higher than that in manual traffic. As a result the vehicle pile-up spills over in section 2 (Fig. 12(c)).

We observe that the presence of semi-automated vehicles does not affect the total travel time during traffic disturbances when we compare the space-time graphs of vehicles in manual and mixed traffic in Fig.13. The 27th vehicle in mixed traffic starts at approximately the same position as the 20th vehicle in manual traffic, and travels 10.6% (covering 365m) more distance than the latter (covering 330m) in 50s. However, this increase is marginal and is within the modeling error.
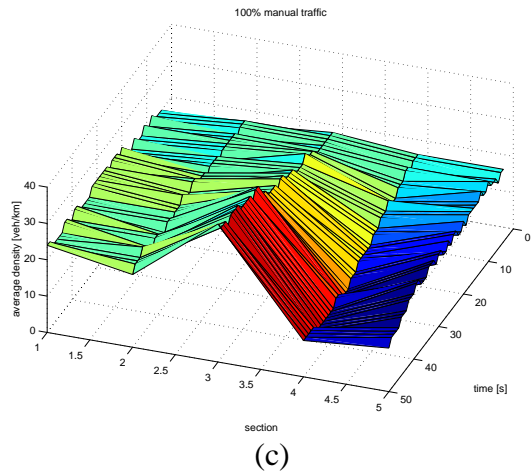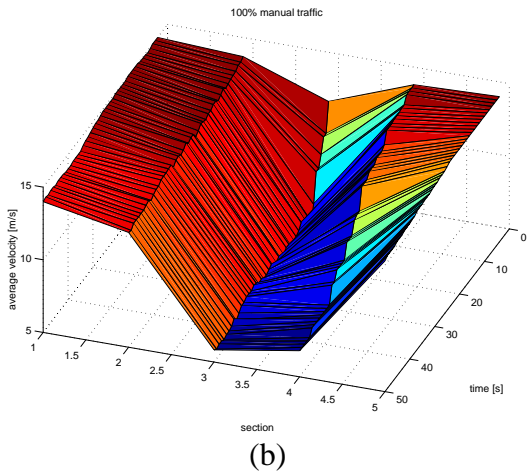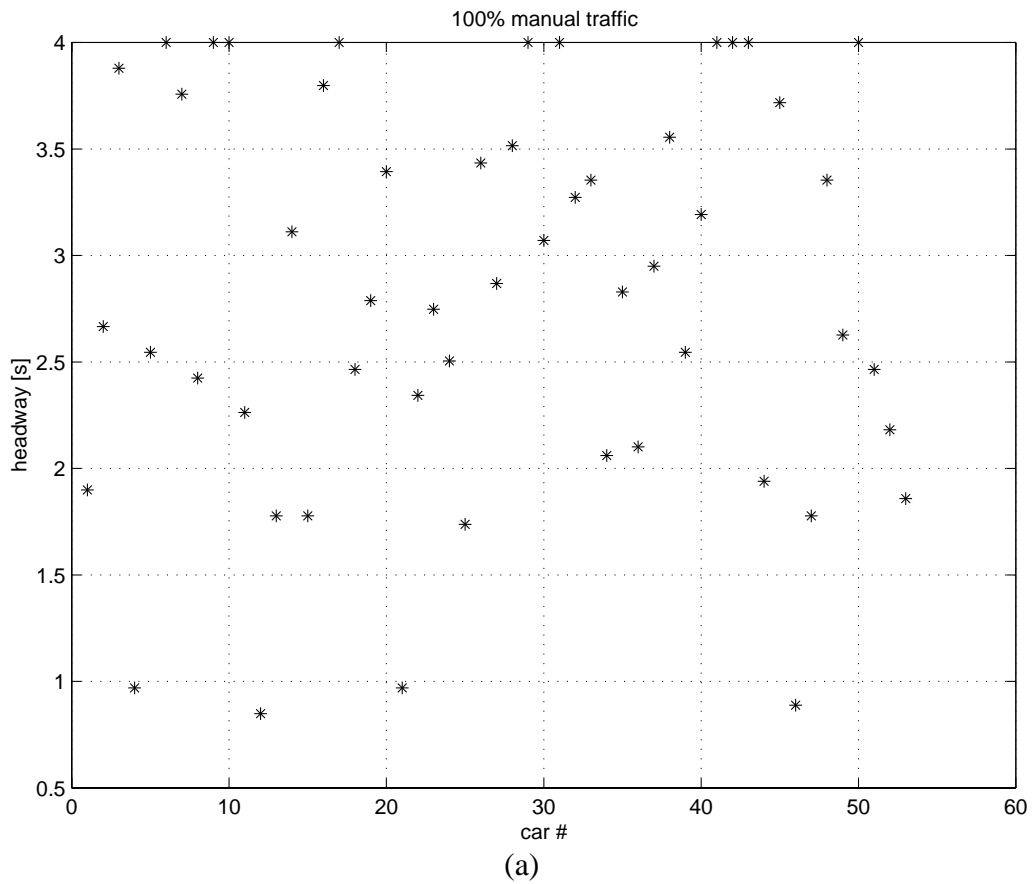
22

(a)

(b)

(c)

Figure 11: Macroscopic behavior of vehicles in 100% manual traffic.
(a) Distribution of Time headway of vehicles.
(b) Average speed distribution of vehicles in 5 sections of the highway.
(c) Traffic density distribution of vehicles in the 5 sections of the highway.

(a)

(b)

(c)

Figure 12: Macroscopic behavior of vehicles in mixed traffic where 50% are semi-
automated vehicles. (a) Distribution of Time headway of vehicles.
(b) Average speed distribution of vehicles in 5 sections of the highway.
(c) Traffic density distribution of vehicles in 5 sections of the highway.

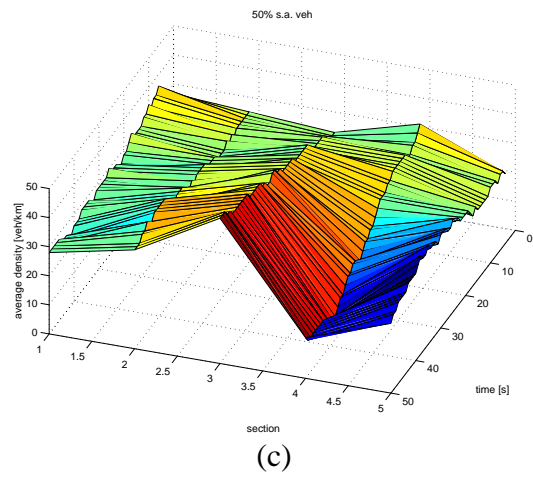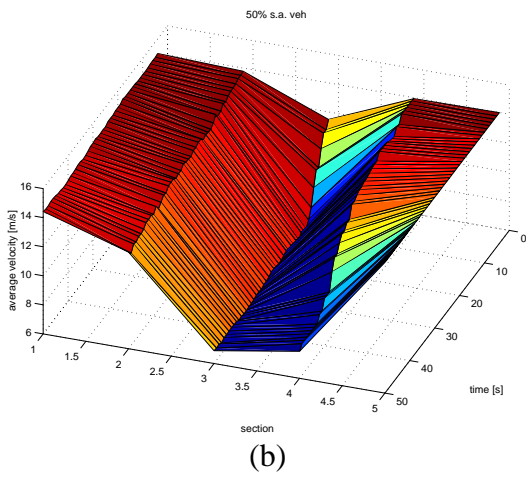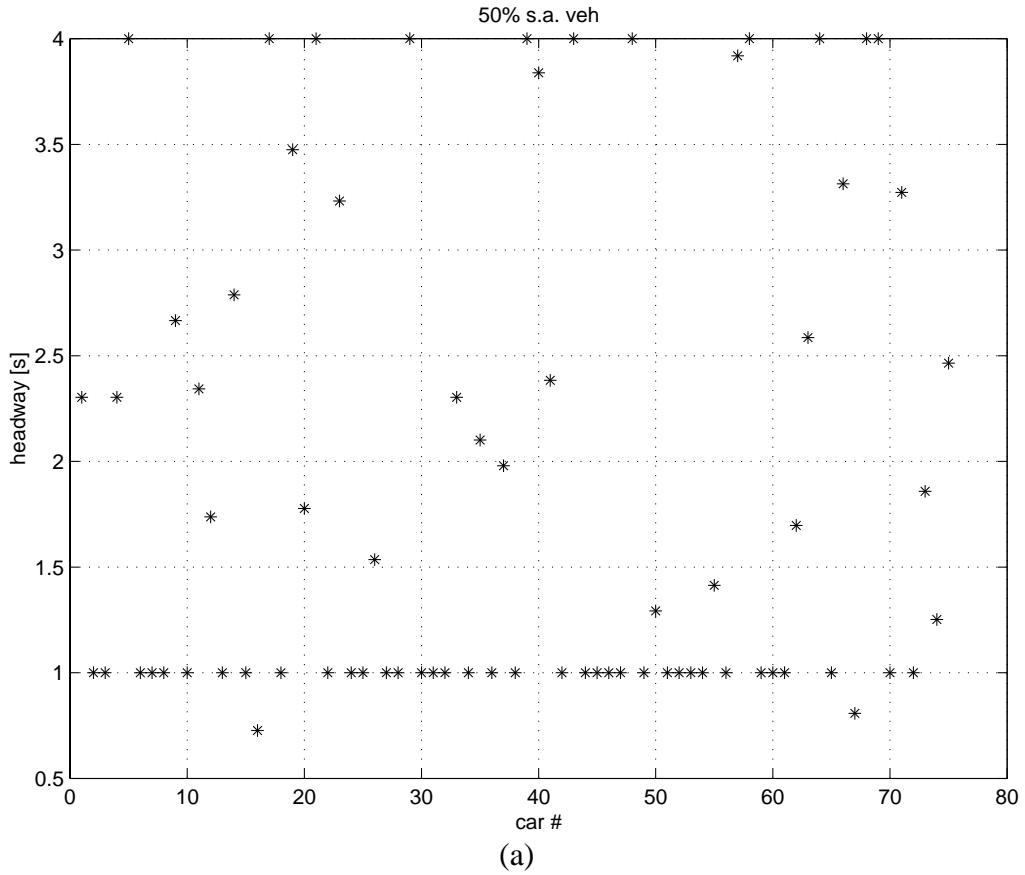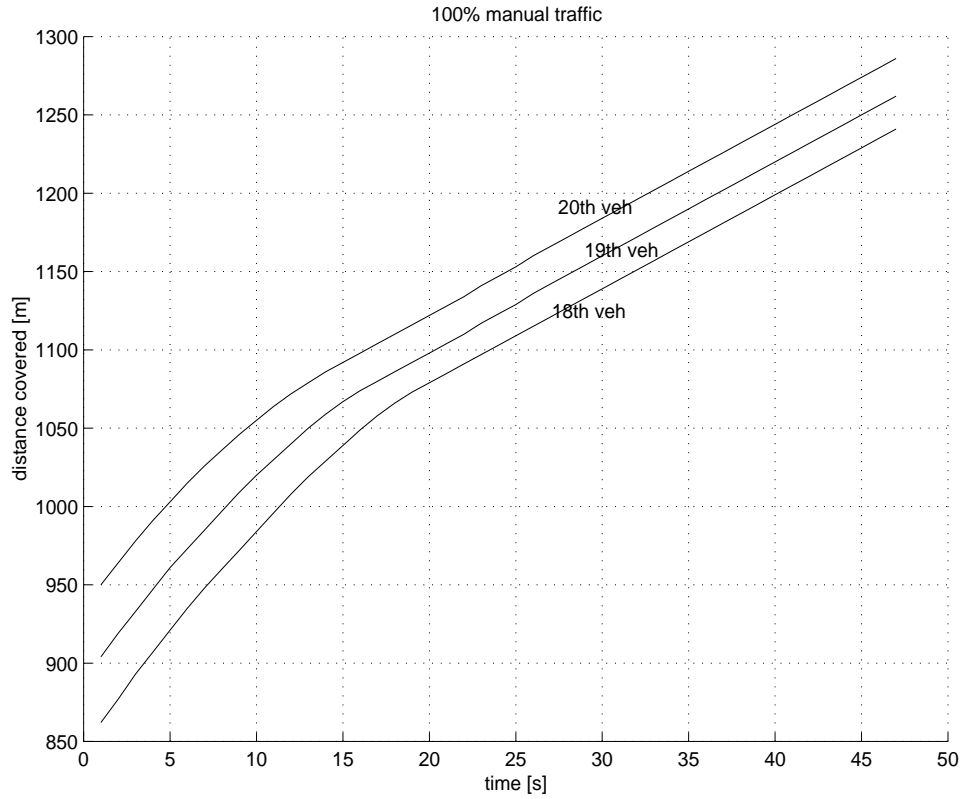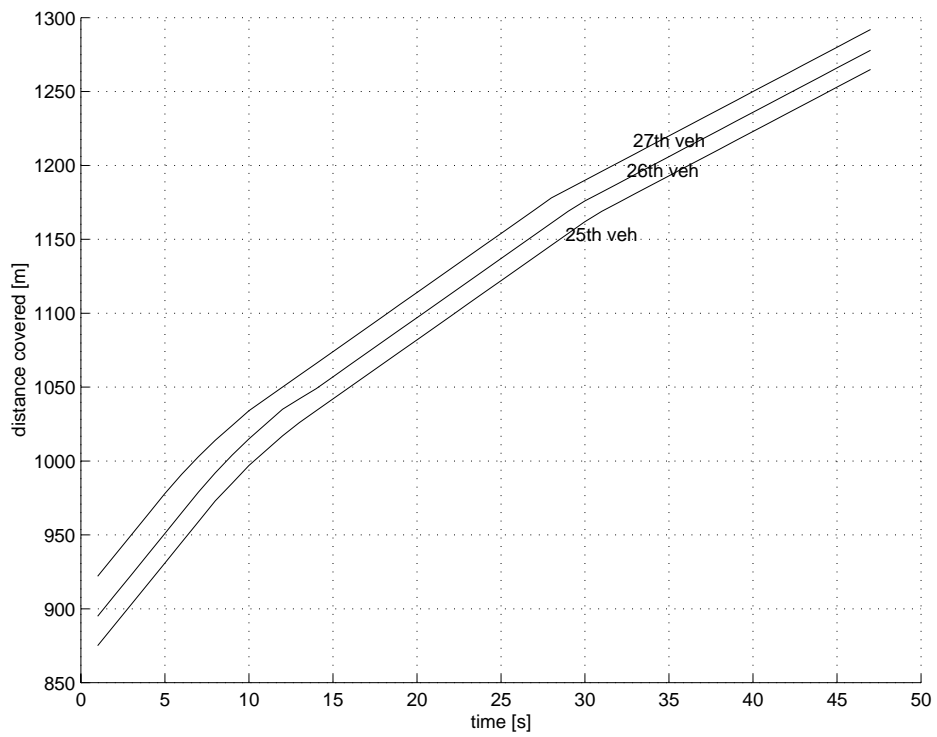Figure 13: Distance covered by vehicles starting at approximately the same place in (a) 100% manual traffic and (b) mixed traffic with 50% semi-automated vehicles.

4 Stop-and-go Traffic

In this Section, we show that the average delay experienced by vehicles on the highway due to stop-and-go conditions is shorter in mixed traffic than in manual traffic. Consider Fig. 14 that shows two shock waves 1-2 and 2-3 that create a stop-and-go condition. The vehicles come to a complete stop after the first shock wave 1-2 as shown in the shaded region 2. Thereafter reaching the second shock wave 2-3 they start moving again. As before, we assume instantaneous acceleration/deceleration of vehicles and vehicles of the same class use identical time headways and spacings at a given state. Consider random vehicle arrivals at the shock wave 1-2 at a rate q_1 per unit time, which is the traffic flow rate in region 1. We take the vehicle discharge rate to be equal to q_2 that represents the traffic flow rate in region 2. The stop-and-go situation can be viewed as a first-come-first-serve system as the first vehicle to stop is the first one to start moving. Therefore, we can model the system as an M/M/1 queue with Poisson arrivals and exponential service rate [10]. The theoretical Poisson distribution model is the most commonly used model for vehicular traffic [18,19]. It gives a "satisfactory fit" with empirical traffic data, even at high traffic flow rates as shown in [19].
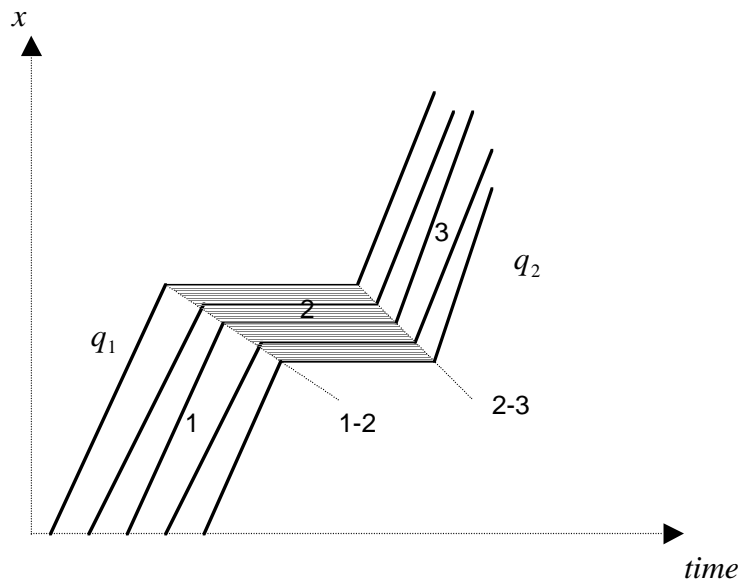

Figure 14: Stop-and-go traffic.

We have the following arrival and service rates

$$\lambda = q_1 \text{ and } \mu = q_2$$

The utilization factor is given by

$$\rho = \frac{\lambda}{\mu} = \frac{q_1}{q_2} \tag{33}$$

26

We assume that $q_2 > q_1$, i.e. $\rho < 1$, which is required for ergodicity [10].

4.1 Manual Traffic

For manual traffic, we have the following:

$$q_1 = k_m v_1 = \frac{v_1}{h_m v_1 + L},$$ where q_1 is the traffic flow rate in region 1, $k_m = \frac{1}{h_m v_1 + L}$ is the traffic density, h_m is the average time headway in manual traffic, v_1 is the average speed of vehicles in region 1 and L is the average length of vehicles.

$$q_2 = k_m v_2 = \frac{v_2}{h_m v_2 + L},$$ where q_2 is the traffic flow rate in region 2 and v_2 is the average speed of vehicles in region 2.

Remark 2: For ergodicity, we have

$$q_2 > q_1$$
$$\Rightarrow v_2 > v_1 \tag{34}$$

The average delay experienced by a vehicle in region 3 due to the stop-and-go condition is given by [10]

$$T_1 = \frac{1/\mu}{1-\rho} = \frac{1}{q_2 - q_1} = \frac{(h_m v_1 + L)(h_m v_2 + L)}{L(v_2 - v_1)} \tag{35}$$

4.2 Mixed Traffic

For mixed traffic we have

$$\bar{q}_1 = k_{mix} v_1 = \frac{v_1}{h_{mix} v_1 + L},$$ where $\bar{q}_1$ is the mixed traffic flow rate in region 1, $h_{mix} = p h_a + (1-p) h_m$ is the average time headway in mixed traffic, h_a is the time headway of semi-automated vehicles and p is the percentage of semi-automated vehicles in mixed traffic.

$$\bar{q}_2 = k_{mix} v_2 = \frac{v_2}{h_{mix} v_2 + L},$$ where $\bar{q}_2$ is the mixed traffic flow rate in region 2.

Therefore, we have the average delay given by

27

$$T_2 = \frac{1/\mu}{1-\rho} = \frac{1}{\overline{q}_2 - \overline{q}_1} = \frac{(h_{mix}v_1 + L)(h_{mix}v_2 + L)}{L(v_2 - v_1)} \tag{36}$$

To show that the average delay experienced by vehicles at standstill in region 3 of Fig. 14 is shorter in mixed traffic than in manual traffic, we need to verify that

$$T_1 - T_2 > 0 \quad \forall p \;\; p \in (0,1) \tag{37}$$

Using (35) and (36) we obtain

$$T_1 - T_2 = \frac{(h_m v_1 + L)(h_m v_2 + L)}{L(v_2 - v_1)} - \frac{(h_{mix}v_1 + L)(h_{mix}v_2 + L)}{L(v_2 - v_1)} \tag{38}$$

The denominator is always positive by (34). The numerator can be expressed as

$$h_m^2 v_1 v_2 + h_m L(v_1 + v_2) - h_{mix}^2 v_1 v_2 - h_{mix} L(v_1 + v_2) \tag{39}$$

which is always positive for all p as $h_m > h_{mix}$ (since $h_m > h_a$ and $0 < p < 1$). Hence (37) is satisfied.

It is interesting to note that though the above phenomenon occurs, the average number of vehicles at standstill remains unchanged in manual and mixed traffic. It is given by [10]

$$\overline{N} = \frac{\rho}{1-\rho} = \frac{v_1}{v_2 - v_1} \tag{40}$$

which is independent of the average intervehicle spacings and hence the type of traffic.

The above results agree with intuition. In the previous Section, we observed that shock waves travel faster in mixed traffic than in manual traffic. Thus the shaded region 3, where the vehicles are at standstill, travels upstream faster in mixed traffic than in manual traffic. This explains (37). However, the relative speed between the two shock waves remains the same in both types of traffic. Thus, the area or the number of vehicles they cover also remains unchanged, which is shown in (40). Furthermore, from the environmental perspective, lower average delay for vehicles in mixed traffic during the presence of shock waves that produce stop-and-go traffic should reduce fuel consumption and air pollution.

5 Conclusion

In this paper, we derive the $q-k$ diagram for mixed traffic using the $q-k$ diagrams for 100% manual and 100% semi-automated vehicle traffic and assuming that semi-automated vehicles use a time headway smaller than current manual traffic average. We show graphically that semi-automated vehicles propagate traffic disturbances such as shock waves faster without affecting the total travel time. Furthermore, we use an M/M/1 queue to show that the average delay experienced by vehicles in mixed traffic is lower than those in manual traffic during shock waves that produce stop-and-go traffic. Based on the macroscopic mixed traffic analysis presented in this paper, we conclude the following results:

- Mixed traffic flow rate is greater than manual traffic flow rate for the same traffic density.
- Mixed traffic $q-k$ curve remains in the region between the $q-k$ curves for 100% manual and 100% semi-automated traffic.
- Presence of semi-automated vehicles in mixed traffic increases the speed of propagation of shock waves without affecting the total travel time.
- Presence of semi-automated vehicles in mixed traffic increases the traffic flow rate and traffic density.
- The average delay experienced by vehicles during stop-and-go conditions is shorter in mixed traffic than in manual traffic while the average number of vehicles at standstill during stop-and-go conditions remains the same in manual and mixed traffic.

References

[1] M.J. Lighthill and G.B. Whitham, "On Kinematic Waves: A Theory of Traffic Flow on Long Crowded Roads", *Proc. of the Royal Society of London,* A229, No. 1178, pp.317-345, 1955.
[2] D.R. Drew, "Traffic Flow Theory and Control", McGraw-Hill Book Co., 1968.
[3] P. Ioannou and T. Xu, "Throttle and Brake Control", *IVHS Journal,* vol. 1(4), pp. 345-377, 1994
[4] M. J. Cassidy, "Traffic Flow and Capacity", *Handbook of Transportation Science,* Ed. Randolph Hall, pp. 151-186, Kluwer Academic Publishers, 1999
[5] S. Cohen, "Traffic Variables", *Encyclopedia of Traffic Flow,* Ed. M. Papageorgiou. Pp.139-143.
[6] A. Bose and P. Ioannou, "Issues and Analysis of Mixed Semi-Automated/Manual Traffic", *SAE Technical Paper Series*, No.981943, 1998
[7] L. A. Pipes, "An Operational Analysis of Traffic Dynamics", *J. of Applied Physics,* vol.24, pp. 271-281, 1953
[8] P. E. Chandler, R. Herman and E. W. Montroll, "Traffic Dynamics: Studies in Car Following", *Operations Research,* vol. 6, pp. 165-184, 1958

[9] R. J. Walker and C. J. Harris, "A Multi-Sensor Fusion System for a Laboratory Based Autonomous Vehicle", *Intelligent Autonomous Vehicles IFAC Workshop*, Southampton U.K., pp. 105-110, 1993.

[10] L. Kleinrock, "Queueing Systems Vol. I: Theory", John Wiley & Sons, 1975.

[11] W. Leutzbach, "Introduction to the theory of traffic flow", Springer-Verlag, 1972.

[12] A. Bose and P. Ioannou, "Analysis of traffic flow with mixed manual and semi-automated vehicles", *Proceedings of American Control Conference*, pp. 2173-2177, 1999.

[13] J.K. Hedrick, D. McMahon, V. Narendran and D. Swaroop, "Longitudinal vehicle controller design for IVHS systems", *Proceedings of American Control Conference,* pp.3107-3112, 1991.

[14] P.A. Ioannou, F. Ahmed-Zaid and D. Wuh, "A time headway autonomous Intelligent Cruise Controller: Design and simulation", Technical Report, USC-SCT 92-11-01, Los Angeles, 1992.

[15] *1985 Highway Capacity Manual*, Transportation Research Board Special Report 209.

[16] I. Chabani and M. Papageorgiou, "Traffic Networks: Flow Modeling and Control", Class notes, MIT, Fall 1997.

[17] L.C. Edie, "Flow Theories", *Traffic Science,* Ed. By D.C. Gazis, John Wiley and Sons, 1974.

[18] D. E. Cleveland and D. G. Capelle, "Queuing Theory Approaches", *An Introduction to Traffic Flow Theory*, Ed. By D. L. Gerlough and D. G. Capelle, Highway Research Board, 1964.

[19] L. C. Edie, "Traffic Delays at Toll Booths", *Journal of the Operations Research Society of America*, vol. 2, No. 2, pp. 107-138, May 1954.

[20] A. Bose and P. Ioannou, "Analysis of Traffic Flow with Mixed Manual and Semi-Automated Vehicles", submitted to IEEE Transactions on Intelligent Transportation Systems, 2000.

[21] D. Swaroop and K. R. Rajagopal, "Intelligent Cruise Control Systems and Traffic Flow Stability", *Transportation Research*, *Part C: Emerging Technologies*, 7(6), pp. 329-352, 1999.